



UNITED NATIONS EDUCATIONAL, SCIENTIFIC AND CULTURAL ORGANIZATION  
INTERNATIONAL ATOMIC ENERGY AGENCY  
INTERNATIONAL CENTRE FOR THEORETICAL PHYSICS  
I.C.T.P., P.O. BOX 586, 34100 TRIESTE, ITALY, CABLE: CENTRATOM TRIESTE



*H4.SMR/994-21*

**SPRING COLLEGES IN  
COMPUTATIONAL PHYSICS**

*19 May - 27 June 1997*

**TIME DEPENDENT METHODS IN  
QUANTUM MECHANICS  
III-IV-V**

**R. COALSON  
University of Pittsburgh  
Department of Physics  
Pittsburgh, Pennsylvania 15260  
U.S.A.**

# Chapt. 3: Multidimensional Gaussian Wavepackets and Quantum Theory of Inelastic Scattering

## 1 Multidimensional Gaussian Wavepacket Dynamics

The (thawed) Gaussian Wavepacket Dynamics (GWD) algorithm can be extended to treat wavepacket dynamics in any number of Cartesian dimensions. As in the 1-d case, the algorithm is exact for potentials which are at most quadratic in the coordinates, and approximate for anharmonic potentials. The quality of the solution degrades with time for the latter class of problems. Fortunately, many experimentally interesting properties reflect only short-time dynamics. Processes in this class include cross sections for simple scattering and photodissociation events, electronic absorption spectra, resonance Raman spectra, and others.

The steps are basically the same as in 1-d, except that vectors and matrices appear in the multidimensional analog. Starting from an initially Gaussian wavepacket, the packet is assumed to remain Gaussian for all times. A general  $N$ -dimensional Gaussian wavepacket may be written in the form:

$$\psi(\vec{x}, t) = e^{\frac{i}{\hbar}[(\vec{x}-\vec{x}_t) \cdot \mathbf{A}_t \cdot (\vec{x}-\vec{x}_t) + \vec{p}_t \cdot (\vec{x}-\vec{x}_t) + \gamma_t]} \quad (1)$$

Here, for an  $N$ -dimensional Hamiltonian, the vectors are obviously  $N$ -dimensional, and  $\mathbf{A}_t$  is an  $N \times N$  symmetric matrix of complex valued parameters. These parameters, as well as those in the real-valued vectors  $\vec{x}_t$ ,  $\vec{p}_t$ , and the complex valued scalar  $\gamma_t$ , evolve in time. To obtain equations of motion for them, the potential energy is expanded through second order in all coordinates around the instantaneous center of the wavepacket  $\vec{x}_t$ , i.e.

$$V(\vec{x}, t) \cong V_0 + \vec{V}_1 \cdot (\vec{x} - \vec{x}_t) + \frac{1}{2}(\vec{x} - \vec{x}_t) \cdot \mathbf{V}_2 \cdot (\vec{x} - \vec{x}_t), \quad (2)$$

$V_0, \vec{V}_1$  and  $\mathbf{V}_2$  being the standard coefficients in a Taylor series expansion of  $V(\vec{x}, t)$  about  $x_t$ . Substitution of the r.h.s. of Eq. (2) and the Gaussian wavepacket in Eq. (1) leads directly to the multidimensional equations of motion for thawed Gaussian wavepacket dynamics [1]:

$$\dot{\vec{x}}_t = \mathbf{m}^{-1} \cdot \vec{p}_t \quad (3)$$

$$\dot{\vec{p}}_t = -\vec{V}_1 \quad (4)$$

$$\dot{\mathbf{A}}_t = -2\mathbf{A}_t \cdot \mathbf{m}^{-1} \cdot \mathbf{A}_t - \mathbf{V}_2/2 \quad (5)$$

$$\dot{\gamma}_t = i\hbar \text{tr} [\mathbf{m}^{-1} \cdot \mathbf{A}_t] + \frac{1}{2} \vec{p}_t \cdot \mathbf{m}^{-1} \cdot \vec{p}_t - V_0, \quad (6)$$

where  $\mathbf{m}$  is an  $N \times N$  diagonal matrix containing the masses associated with each cartesian coordinate. These equations of motion have the same general structure as in the 1-d case. Namely,  $\vec{x}_t$ ,  $\vec{p}_t$  obey Hamilton's (Newton's) equations, while auxiliary 1st order differential equations prescribe the update of the spread matrix  $\mathbf{A}_t$  and phase/norm parameter  $\gamma_t$ .

## 2 Quantum Scattering Theory with Internal Degrees of Freedom: Inelastic Collisions

Consider the collinear oscillator-projectile problem introduced in Chapt. 1. For concreteness, we shall take the oscillator to be of harmonic type. [The case of an anharmonic oscillator is considered in Chapt. 4.] The relevant quantum Hamiltonian (known as the Secrest-Johnson Hamiltonian) reads:

$$\hat{H} = \frac{-1}{2m_x} \partial_x^2 + \frac{-1}{2m_y} \partial_y^2 + \frac{1}{2} kx^2 + Ae^{-\kappa(y-x)} \quad (7)$$

[ $\hbar = 1$  in this section.] We ask the fundamental question: Given  $m_y$  incident with well defined momentum  $k_i$  (hence kinetic energy  $\mathcal{E}_i = k_i^2/2m_y$ ), and  $m_x$  in an eigenstate  $\phi_i$  of the uncoupled harmonic oscillator Hamiltonian (i.e., Eq. (7) with the y-kinetic energy and the interaction potential removed) corresponding to vibrational energy eigenvalue  $\epsilon_i$ , what is the probability that  $m_y$  exits with kinetic energy  $\mathcal{E}_f = \mathcal{E}_i + (\epsilon_i - \epsilon_f)$ , leaving the oscillator in  $\phi_f$  corresponding to vibrational energy  $\epsilon_f$ ?

Essentially, the desired transition probabilities are squares of coefficients ("S-matrix amplitudes") in the eigenfunctions of the full two-dimensional scattering Hamiltonian (7). The underlying theory is somewhat complicated, partly because the eigenstates corresponding to a given total energy are degenerate, and one must decide what linear combination of eigenstates is appropriate ("scattering boundary conditions"). This "S-matrix theory" can be translated into wavepacket propagation language, and the result is mathematically simple, conceptually natural, and computationally useful. Denoting the probability to make the

transition described in the previous paragraph as  $|S_{fi}(E)|^2$ , where  $E$  is the total (conserved!) energy in the system:

$$\mathcal{E}_i + \epsilon_i = E = \mathcal{E}_f + \epsilon_f ,$$

then:

$$|S_{fi}(E)|^2 = \frac{k_i(E)}{k_f(E)} \left| \frac{\int_{-\infty}^{\infty} dx \int_{-\infty}^{\infty} dy \phi_f(x) e^{-ik_f(E)y} \psi(x, y, T)}{\int_{-\infty}^{\infty} dx \int_{-\infty}^{\infty} dy \phi_i(x) e^{ik_i(E)y} \psi(x, y, -T)} \right|^2 \quad (8)$$

Here  $T$  is a (long) time interval. The wavepacket begins at  $t = -T$  as a factorized packet of the form:

$$\psi(x, y, -T) = \phi_i(x) G_{in}(y) \quad (9)$$

where  $G_{in}(y)$  is a wavepacket moving *towards* the target. In principle the details of  $G_{in}(y)$  are rather arbitrary. In practice  $G$  is taken to be a Gaussian for simplicity. A more substantive restriction is to choose the average momentum in the superposition of plane waves which comprise the incident Gaussian to be in the range of energies at which the S-matrix is desired. Again, in principle a single wavepacket can be used to extract the  $i$ 'th column of the S-matrix at all energies, but in practice accurate results will be obtained only in the energy region where the incident projectile wavepacket is well represented.

There are two other practical details worth mentioning here. First, there is a useful property of the exact solution, namely “unitarity”, which should be monitored in computational work. The unitarity condition is simply  $\sum_f |S_{fi}(E)|^2 = 1$ , where the sum is over all open channels at energy  $E$  (an “open” channel being a final vibrational state which is accessible at that energy).

A second practical detail is that it is best to choose the incident translational wavepacket  $G_{in}(y)$  in such a way that the packet narrows or “focusses” as it enters the collision region. It is always desirable to have narrow wavepackets in the interaction region. Even for exact grid codes, this keeps the packet well contained in the center of the grid and the collision event crisply defined.

Note that a single wavepacket contains a lot of S-matrix information. The entire  $i$ 'th column of the S-matrix can be extracted over a range of energies (depending on the construction of  $G_{in}(y)$ ).

A 2-d grid integrator of the type introduced in Chapt. 2 above can be used to extract exact S-matrix elements for the Secrest-Johnson potential. These results can be compared to those

obtained via Gaussian Wavepacket Dynamics, as shown in Fig. 1. The comparison is quite favorable, even at relatively low collision energies where the applicability of the assumptions of GWD is more suspect.

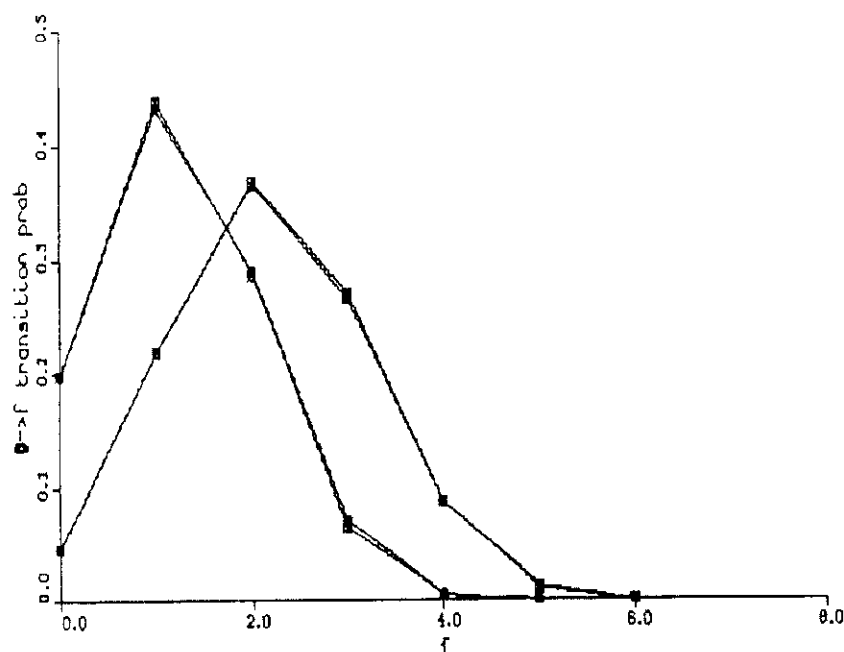


Figure 1: Probabilities for  $0 \rightarrow f$  transition at energies  $E = 8, 10$  are shown for the Secrest-Johnson Hamiltonian with parameters  $\hbar = m_x = 1, m_y = 2/3, k = 1, A = 10, a = 0.3$ . At each energy exact results [1, 2] are compared to results extracted from a GWD trajectory. The agreement is very good.

## References

- [1] E.J. Heller, J. Chem. Phys. **62**, 1544 (1975); Accts. Chem. Res. **14**, 368, 1981.
- [2] D. Secrest and B.R. Johnson, J. Chem. Phys. **45**, 4556 (1966).

# Chapt. 4: The Time-Dependent Hartree Approximation and Configuration Interaction

## 1 The Time-Dependent Hartree Approximation

A useful approximate technique for propagating wavepackets is the Time-Dependent Hartree (TDH) method. In this scheme the wavepacket is approximated as a factorized packet, one for each degree of freedom. For concreteness, let us consider a system with two degrees of freedom  $x$  and  $y$ . The Hamiltonian is taken to be of the form:

$$\hat{H} = \hat{h}_x + \hat{h}_y + V_{int}(x, y) , \quad (1)$$

with  $\hat{h}_x$  a “single-particle” Hamiltonian that depends on variable  $x$ . Typically it has the structure  $\hat{h}_x = \hat{T}_x + v_x(x)$ , where  $\hat{T}_x$  is the appropriate 1-d kinetic energy operator and  $v_x(x)$  is a “single-particle” potential function that depends only on position  $x$ .  $\hat{h}_y$  is defined analogously.  $V_{int}$  is the interaction potential that couples the motion of the two degrees of freedom. In the TDH approximation the system wavepacket  $\psi(x, y, t)$  is replaced by:

$$\psi(x, y, t) = e^{iS(t)} \phi_x(x, t) \phi_y(y, t) \quad (2)$$

Here  $S(t)$  is a real phase factor given by

$$S(t) = \int dx \int dy |\phi_x(x, t)|^2 |\phi_y(y, t)|^2 V_{int}(x, y) ,$$

which has been extracted to simplify the equations of motion for  $\phi_{x,y}$  presented in the next paragraph. [In this chapter  $\hbar = 1$  and all spatial integrals run from  $-\infty$  to  $+\infty$  unless otherwise noted.]

The TDH equations of motion are derived by appealing the Dirac-Frenkel-McLachlan variational principle [1]. One finds that the packet  $\phi_x(x, t)$  obeys a 1-d TDSE with an effective time dependent potential that reflects its coupling to the  $y$ -coordinate. Specifically:

$$i\partial\phi_x(x, t)/\partial t = \left[ \hat{h}_x + \int dy |\phi_y(y, t)|^2 V_{int}(x, y) \right] \phi_x(x, t) \quad (3)$$

and analogously for  $\phi_y(y, t)$ . The interpretation of the effective driving potential on each coordinate is simple and physically appealing. For example, the  $x$ -coordinate “feels” a potential which is the average of the full interaction potential over the instantaneous probability

distribution of the y-particle. This is the “best” way that one can attempt to describe the dynamics using a single-particle factorization ansatz. It is often termed a “mean field” or “self-consistent field” approximation.

There are many nice features of TDH quantum dynamics. It represents a tremendous reduction of computational effort as the dimensionality of the system grows in comparison to an exact solution using grid methods. The scaling of effort (both cpu and storage) grows essentially linearly with spatial dimension in the TDH case, while it grows exponentially for exact grid-propagation algorithms. Since the full wavepacket factors into 1-d pieces in the TDH approximation, integrals needed to “project out” measurable quantities (transition probabilities, scattering and spectroscopic cross sections, etc.) are immediately tractable for large-dimensional systems. The approximation conserves both norm and, for time independent systems, average energy  $\langle \hat{H} \rangle$ ; maintaining these properties is beneficial to both stability and accuracy. Physically, the procedure is particularly appealing in an event like a collision, where  $V_{int} \rightarrow 0$  at long times, so the TDH solution becomes asymptotically stable (does not degrade after the collision is over). In general, if the interaction between degrees of freedom is confined to a short time period, the use of TDH is naturally suggested.

In the wake of this enthusiasm, we should not lose sight of the fact that TDH *is* an approximation. From the discussion above we can summarize the approximation as “neglect of direct correlation” (direct correlation is essentially the degree to which the full system wavefunction cannot be factorized a la TDH). Nevertheless, TDH has been widely successful for studying short-time (subpicosecond) dynamics in many-dimensional quantum systems.

To give a simple example which illustrates the utility of TDH, consider again the collinear scattering model of Chapt. 3, but with a *Morse* rather than a harmonic oscillator. This gives problems for GWD, not so much due to difficulties treating the collision itself, but due to breakdown of GWD in an isolated Morse potential. The approximation must be able to account for this motion for some time (typically several vibrational periods) before and after the collision. As we saw in Chapter 1, GWD cannot always do this successfully (depending on anharmonicity of the Morse well, initial conditions, degree of excitation imparted by collision, etc.). The TDH approximation, however, is exact before and after the collision, so its only inaccuracies are those accumulated during the collision event. We might expect it to be successful in extracting S-matrix elements for this problem. Indeed, a numerical example illustrating the utility of TDH dynamics for the collinear atom-Morse collision system is shown in Fig. 1. The Hamiltonian is the same as the Secrest-Johnson Hamiltonian except that the harmonic oscillator potential is replaced by the Morse potential  $D(1 - e^{-\alpha x})^2$ .

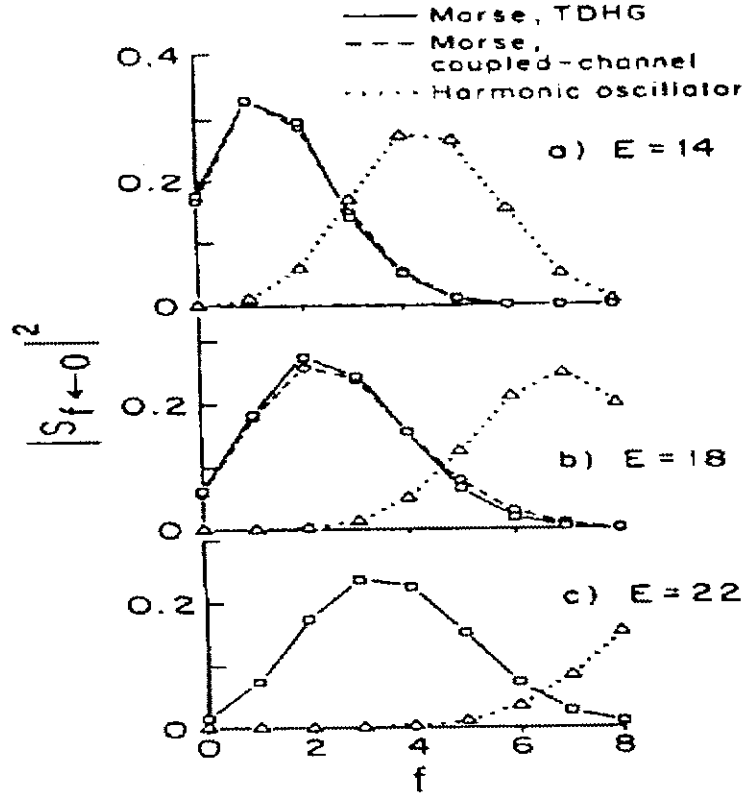


Figure 1: Probabilities for  $0 \rightarrow f$  transition in a Morse oscillator after collision with an atom at total energies  $E = 14, 18, 22$  are shown in panels (a), (b), (c), respectively. System parameters are  $\hbar = m_x = 1$ ,  $D = 20$ ,  $\alpha = 0.158$ ,  $m_y = 2/3$ ,  $a = 0.3$ ,  $V_0 = 1$  (see Ref. [2] for full details). TDH results are marked with squares, exact numerical results via circles. Results for the equivalent harmonic oscillator system (based on the curvature at the bottom of the Morse well) are shown via triangles.

## 2 Beyond TDH: Configuration Interaction

It is natural to consider the possibility that TDH can be used as a zeroth order approximation whose inadequacies can be corrected with additional effort. Configuration Interaction is one such strategy. It has a well-known analog in the quantum theory of molecular electronic structure, where the Hartree-Fock approximation plays the role that TDH plays in the quantum dynamics of atomic/molecular nuclei.

The first step is to “build” an orthogonal basis of wavefunctions upon the chosen initial state. In our applications to 2-d scattering problems, we have considered states of the form  $\phi_i(x)G_{in}(y)$ , where  $G_{in}$  is a (moving) Gaussian wavepacket and  $\phi_i(x)$  a vibrational eigenstate



of an appropriate 1-d potential well. So, the initial single-particle basis functions in the  $x$  coordinate are simply the eigenfunctions of the isolated oscillator Hamiltonian. Let us denote the  $j$ 'th member of this set as  $\psi_x^{(j)}$ .

For the  $y$ -coordinate, we can easily construct excited states that are orthogonal to the Gaussian packet  $G$ . Note that  $|G(y, -T)|^2 = N_0^2 \exp[-2Im\alpha_{-T}(y - y_{-T})^2]$ , where  $N_0$  is a normalization constant so that this function has unit area. Thus, the set of Hermite-Gaussian functions

$$\psi_y^{(k)}(y) = \frac{1}{\sqrt{2^k k!}} H_k[2Im\alpha_{-T}(y - y_{-T})] G(y, -T) \quad (4)$$

where  $H_k$  is the  $k$ 'th Hermite polynomial, provides such a complete, orthonormal set.

One's first impulse might be to propagate each of the initial basis functions  $\psi_{jk}(x, y) = \psi_x^{(j)}(x)\psi_y^{(k)}(y)$  in time under the TDH approximation, then form a travelling basis set

$$\Psi(x, y, t) = \sum_{jk} a_{jk}(t) \psi_{jk}(x, y, t) ,$$

where the  $a_{jk}(t)$  are superposition functions that are determined by substituting the (in principle, complete) expansion for  $\Psi(x, y, t)$  into the full 2-d Schrodinger equation. Indeed, one then finds a set of 1st order linearly coupled evolution equations for the  $\vec{a}(t) = (a_{00}(t), a_{10}(t), a_{01}(t) \dots)$  which has the form:

$$i\mathbf{S}(t)\dot{\vec{a}}(t) = \mathbf{H}(t)\vec{a}(t) \quad (5)$$

Here, if there are  $N$  total basis functions, then  $\mathbf{S}(t)$  and  $\mathbf{H}(t)$  are  $N \times N$  matrices.  $\mathbf{H}$  reflects the difference between effective TDH and exact Hamiltonian operators (sandwiched between TDH basis functions; cf. below).  $\mathbf{S}$  is a time-dependent matrix of overlaps between TDH basis functions. A problem with this strategy is that the overlap matrix is time-dependent, and, worse, columns can become linearly dependent on each other, which renders inversion of  $\mathbf{S}$  unstable. The origin of the linear dependency problem is the *independent* propagation of each TDH basis function. These functions do not remain orthogonal, as is clear from the preceding remarks.

One solution is to propagate *all* members of the initial basis set using the same effective separable potential. The latter is chosen by propagating one initial product basis function in the set under TDH, then using this time-dependent *separable* potential  $V_{eff}(x, y, t)$  to guide all the members of the 2-d basis. This ensures that all members remain orthonormal for all

times. The evolution equations for the Configuration Interaction (CI) coefficients then take the simple form:

$$i\dot{\vec{a}}(t) = \mathbf{H}(t)\vec{a}(t) \quad (6)$$

with

$$\mathbf{H}_{jk,j'k'}(t) = \langle \psi_{jk}(t) | V(x, y) - V_{eff}(x, y, t) | \psi_{j'k'}(t) \rangle, \quad (7)$$

$V(x, y)$  being the full 2-d potential (sum of all single particle potential plus interaction potential terms). This set of equations is simple and stable to integrate. In the large  $N$  limit, it generates an exact solution of the TDSE for the full 2-d problem.

This CI scheme has been used successfully in a number of applications to molecular scattering and spectroscopy. Note that if the interaction potential is only nonzero during a finite time interval, the basis coefficients  $\vec{a}(t)$  will achieve stable steady state values after the interaction between degrees of freedom is over.

Fig. 2 presents results from an application to 2-d atom-Morse oscillator inelastic scattering which illustrates the principles outlined above.

## References

- [1] See, for example, E.J. Heller, J. Chem. Phys. **64**, 63 (1976).
- [2] R.D. Coalson, Chem. Phys. Lett. **165**, 443 (1990).
- [3] J. Campos Martinez and R.D. Coalson, J. Chem. Phys. **93**, 4740 (1990).

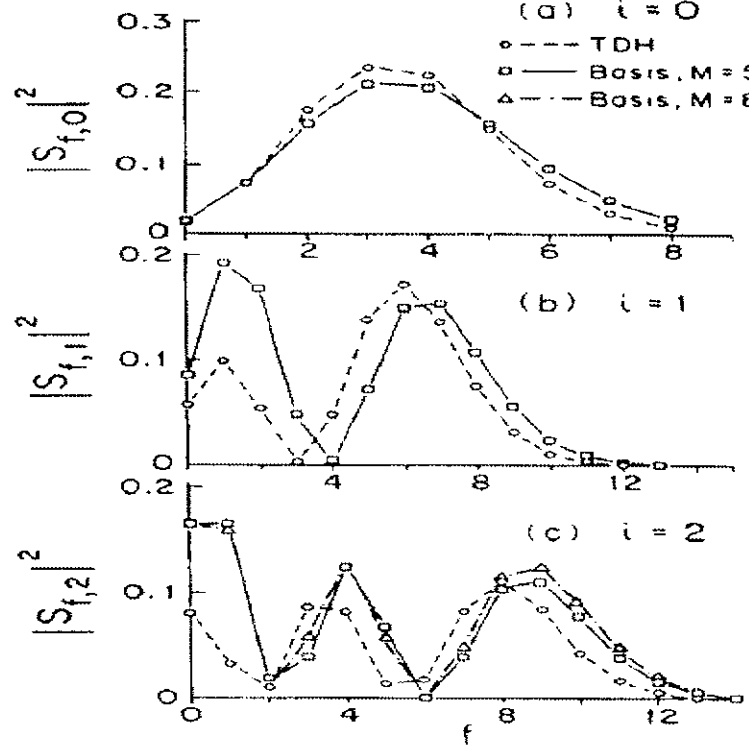


Figure 2: Probabilities for  $i \rightarrow f$  transition in a Morse oscillator after collision with an atom at total energy  $E = 22$  are shown for  $i = 0, 1, 2$  in panels (a), (b), (c), respectively. System parameters are  $\hbar = m_x = 1$ ,  $D = 20$ ,  $\alpha = 0.158$ ,  $m_y = 2/3$ ,  $a = 0.3$ ,  $V_0 = 1$  (see Ref. [3] for full details). TDH results are marked with circles. TDCI results are shown for two basis sets using squares ( $M=5$ ) and triangles ( $M=8$ ), the value of  $M$  indicating the basis size ( $M = \text{number of basis functions in each degree of freedom}$ ; again, see Ref. [3] for full details).

## Chapt. 5: Curve Crossing

### 1 Curve-Crossing in Quantum Dynamics

A wide variety of quantum dynamical phenomena in molecules involve motion on nonadiabatically coupled potential surfaces. The coupling occurs by several mechanisms including spin-orbit coupling (which leads to “intersystem crossing”) and break-down of the Born-Oppenheimer approximation (which leads to “internal conversion”). In such situations, there are nuclear wavepackets associated with several potential surfaces, and a packet starting on one surface, corresponding to preparation in a particular nuclear configuration *and* a particular electronic state (e.g., singlet vs triplet in the case of intersystem crossing), can leak partially or totally onto another potential surface.

A prototypical representative Hamiltonian for such problems is

$$\hat{H} = |1\rangle\langle 1|\hat{h}_1 + |2\rangle\langle 2|\hat{h}_2 + \hat{g}(|1\rangle\langle 2| + |2\rangle\langle 1|) \quad (1)$$

Here  $|1, 2\rangle$  are (structureless) electronic states,  $\hat{h}_{1,2}$  are nuclear coordinate Hamiltonians corresponding to single potential energy surfaces and  $\hat{g}$  is the nonradiative or “nonadiabatic” coupling operator. The nuclear coordinate Hamiltonians have the form  $\hat{h}_j = \hat{T} + \hat{V}_j$ , where  $\hat{T}$  is the kinetic energy operator and  $\hat{V}_j$  the potential surface corresponding to electronic state  $j = 1, 2$  (which is a known function of the nuclear coordinate configuration). The dimensionality of the nuclear coordinate space and the choice of coordinate system (cartesian, curvilinear...) are arbitrary. The nuclear coordinate operator  $\hat{g}$  is taken to be an arbitrary function of nuclear coordinates. The corresponding wavepacket states associated with the Hamiltonian in Eq. (1) are

$$|\Psi(t)\rangle = \phi_1(x, t)|1\rangle + \phi_2(x, t)|2\rangle \quad (2)$$

Here  $\phi_{1,2}(x, t)$  are the nuclear coordinate wavepackets associated with electronic states 1, 2. We note that they depend on nuclear coordinate configuration (which will be multidimensional in general) and time. The time-dependent Schrödinger Equation which governs the dynamics of two coupled wavepackets is (with  $\hbar = 1$ ):

$$i\frac{\partial}{\partial t}|\Psi(t)\rangle = \hat{H}|\Psi(t)\rangle \quad (3)$$

For clarity, it is worthwhile to express the content of Eqs. (1)-(3) in an explicit matrix/vector form:

$$i \begin{bmatrix} \dot{\phi}_1(x, t) \\ \dot{\phi}_2(x, t) \end{bmatrix} = \begin{bmatrix} \hat{h}_1 & g(\hat{x}) \\ g(\hat{x}) & \hat{h}_2 \end{bmatrix} \begin{bmatrix} \phi_1(x, t) \\ \phi_2(x, t) \end{bmatrix} \quad (4)$$

The elements of the Hamiltonian matrix on the r.h.s. of Eq. (4) are all operators on nuclear coordinates.

## 2 Grid Algorithms for Wavepacket Propagation on Two or More Surfaces

Exact grid propagation methods can easily be adapted to treat curve-crossing problems that involve two or more potential surface. Effort scales linearly with the number of coupled surfaces for a fixed spatial dimensionality.

We shall describe the modifications needed to adapt the the SOD method to treat the two-surface case. (The generalization to 3 or more surfaces should then be readily apparent. The Split-Operator method can also be adapted in a straightforward way.)

The SOD analysis proceeds as in the single surface case (subtract  $|\Psi(t-\epsilon)\rangle$  from  $|\Psi(t+\epsilon)\rangle$ ). Specializing to the case of one spatial dimension for simplicity of presentation, we find the following update equation for  $\phi_1(x, t)$ :

$$\frac{i}{2\epsilon} [\phi_1(x_j, t + \epsilon) - \phi_1(x_j, t - \epsilon)] = \hat{h}_1 \phi_1(x_j, t) + g(x_j) \phi_2(x, t) \quad (5)$$

where the operation  $\hat{h}_1 \phi_1(x_j, t) = (\hat{T} + \hat{V}_1) \phi_1(x_j, t)$  is carried out exactly as in the single surface case treated in Chapt. 2. An analogous update equation holds for  $\phi_2$ . It is clear from Eq. 5 and the corresponding equation for updating  $\phi_2$  that in general (unless  $g(x) = 0$ ) amplitude on surface 1 will be transferred to surface 2 and vice-versa. Experimental measurements on both collision induced and spectroscopic properties are sensitive to the details of this dynamics in molecular systems that feature nonadiabatic coupling.

To give a simple illustration, we show results of calculations of dissociation cross sections in a one degree of freedom model of molecular photodissociation. For concreteness, imagine a diatomic molecule which has two nonadiabatically coupled, and repulsive, excited states, as depicted in Fig. 1. Photoexcitation from a lower-lying ground electronic state then results in dissociation into atomic fragments. Neglecting rotation, the internuclear coordinate is  $x$ .

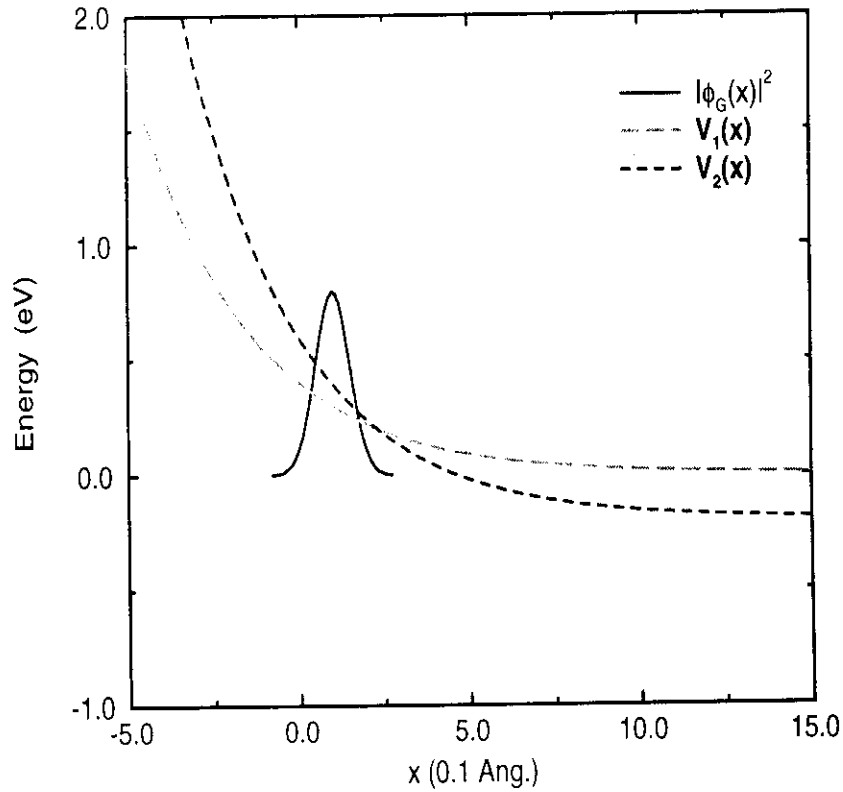


Figure 1: Potential energy functions and initial probability density (associated with preparation on a lower-lying ground state potential) for direct diatomic dissociation on nonadiabatically coupled excited state potential surfaces.  $x$  is the relative coordinate in the diatomic system. The nonadiabatic coupling function is not shown. See Ref. [1] for further details.

Photodissociation is a “half-collision” analog of a molecular scattering process. Instead of starting asymptotically far from the target, moving in for the collision, then moving away from it, in photodissociation the molecule is instantaneously placed in the “collision” or interaction region by photoexcitation. It then proceeds to fall apart (analogous to the second half of a collision event). Although we shall not derive these results, it is reasonable that the following procedure should be used to calculate photodissociation cross sections. Namely, propagate the initially excited wavepacket out of the interaction region into the asymptotic region (corresponding to fragmentation). Then, by appropriate projection onto asymptotic eigenstates (analogous to the numerator in Eq. (8) of Chapt. 3) partial fragment cross sections can be calculated. The wavevector of the plane waves utilized for the asymptotic projection in the photodissociation coordinate is related to the incident frequency of the photexcitation laser in a straightforward way (essentially, “energy conservation”; see Ref.

[1] for details).

In the case of two coupled potential surfaces, asymptotic projections are done on both surfaces to determine the probability that products emerge on *either* surface at a given photoexcitation frequency. For a 1-d photodissociation process such as featured here, there are no internal coordinates like the  $x$  vibrational coordinate studied at length above and hence no further partitioning of fragments by final internal states. A typical result for photodissociation cross sections for the diatom photodissociation model considered here is shown in Fig. 2. Exact results for this problem were obtained by a 1-d wave packet grid integration algorithm.

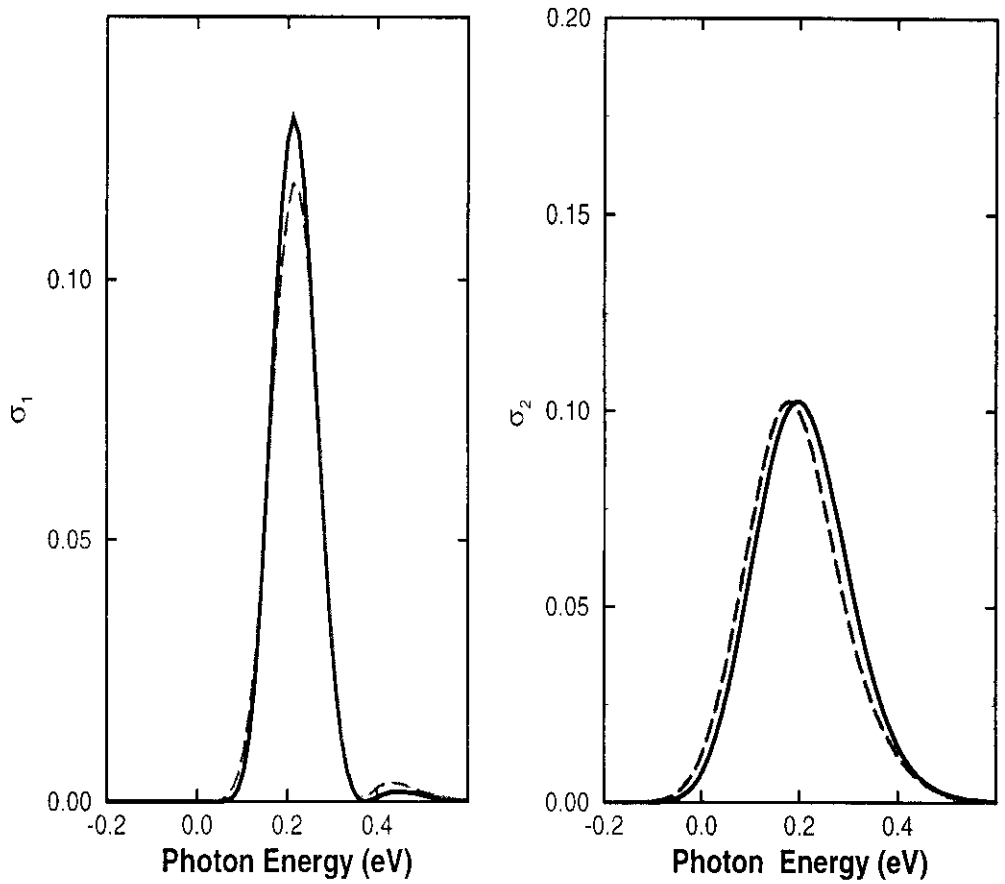


Figure 2: Cross section for photodissociation onto potential surface 1, 2 vs laser excitation energy are shown in left, right panels, respectively, for the molecular system schematized in Fig. 1. Dashed line was obtained using (exact) wavepacket grid integrator, solid line by an approximate Gaussian Wave Packet/Path Integral method. See Ref. [1] for full details.

## References

- [1] R.D. Coalson, J. Phys. Chem. **100**, 7896 (1996).